

Characterizing past and future trend and frequency of extreme rainfall in urban catchments: a case study

Philip Mzava^{a,*}, Patrick Valimba^b and Joel Nobert^b

^a Department of Water Resources Engineering, Water Institute, P.O. Box 35059, Dar es Salaam, Tanzania

^b Department of Water Resources Engineering, College of Engineering and Technology, University of Dar es Salaam, P.O. Box 35131, Dar es Salaam, Tanzania

*Corresponding author. E-mail: pmzava@gmail.com

Abstract

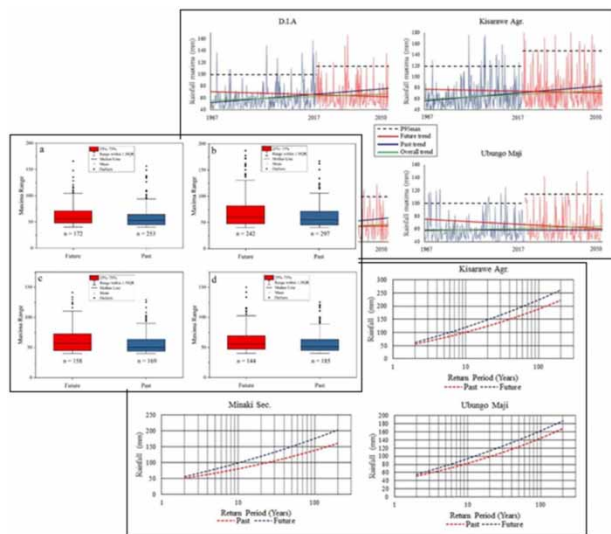
Urban communities in developing countries are one of the most vulnerable areas to extreme rainfall events. The availability of local information on extreme rainfall is therefore critical for proper planning and management of urban flooding impacts. This study examined the past and future characteristics of extreme rainfall in the urban catchments of Dar es Salaam, Tanzania. Investigation of trends and frequency of annual, seasonal and extreme rainfall was conducted, with the period 1967–2017 taken as the past scenario and 2018–2050 as the future scenario; using data from four key ground-based weather stations and RCM data respectively. Mann–Kendall trend analysis and Sen’s slope estimator were used in studying changes in rainfall variability. Frequencies of extreme rainfall events were modeled using the Generalized Pareto model. Overall, the results of trend analysis provided evidence of a significant increase in annual and seasonal maximum rainfall and intensification of extreme rainfall in the future under the RCP4.5 CO₂ concentration scenario. It was determined that extreme rainfall will become more frequent in the future, and their intensities were observed to increase approximately between 20 and 25% relative to the past. The findings of this study may help to develop adaptation strategies for urban flood control in Dar es Salaam.

Key words: Dar es Salaam, EVT, frequency analysis, Mann-Kendall, RCM

Highlights

- Investigate temporal variability in annual, seasonal and extreme rainfall.
- Compare past and future extreme rainfall trend magnitudes based on CORDEX-Africa RCM under RCP 4.5.
- Illustrate the influence of data composition or decomposition on long-term trend results.
- Investigate changes in the historical and projected intensities of extreme rainfall.
- Compute and compare the return levels of extreme rainfall for the past and future scenarios.

Graphical Abstract



INTRODUCTION

In recent decades, changes in climate have been evident all around the globe and the related impacts on the environment, societies, and economies have been significant (IPCC 2013). The behavior of natural extreme phenomena, e.g. heavy rains, floods, drought, etc., have been studied for an extended period of time in different parts of the world, including the UK (Otto 2017), Canada (Li *et al.* 2018), India (Gautam & Bana 2014), Tanzania (Kijazi & Reason 2009; Cioffi *et al.* 2016), United States (Mallakpour & Villarini 2015), South Africa (Nangombe *et al.* 2018), Czech Republic (Elleder 2015), etc. All these studies show the importance of understanding the changes in climate extremes and related effects locally, regionally and globally. Developing countries are more vulnerable to climate change and variability due to their low capacity in adaptivity and therefore the implications of changes in climate variables are mostly detrimental (Gebrechorkos *et al.* 2019a).

Similarly, understanding the characteristics of historical and future extreme rainfall is important while trying to explain the increased cases of flooding in the Dar es Salaam urban area of Tanzania in recent years (2007, 2011, 2014, 2015, 2018 and 2019) while also trying to foresee the flooding conditions in the future. It is also crucial to try to relate any similarities and/or deviations in trends between local, regional and global extreme events while attempting to study global climate change. Although flooding in the Dar es Salaam urban area can be attributed to various factors, including lack of stormwater drainage system, river valley encroachment, poor dumping of solid waste, etc. (Sakijege *et al.* 2012), rainfall remains the major driving force for surface runoff generation. Assessing the changes in extreme rainfall (both past and future) in the Dar es Salaam urban area is of great importance since events of extreme rainfall in the region are directly linked to flooding, property damage, and potential loss of life. Among the top ten natural disasters that threaten the economy of Tanzania, flooding ranks second after epidemics (Ngailo *et al.* 2016). Since Dar es Salaam has the highest population density in Tanzania (approximately 3,133 people/km²), cases of extreme rainfall and flooding have proven to be fatal in the past. Households' losses following the floods of April 2018 in Dar es Salaam were estimated to be over 100 million USD; representing 2–4% of the region's gross domestic product (Erman *et al.* 2019).

General Circulation Models (GCMs) are usually used for modeling earth system components, their interactions and projecting future climate under different greenhouse gas emission scenarios. The application of GCMs in simulating future precipitation extremes is known to be of poor quality.

This is due to their coarse spatial resolution ($>100 \text{ km}^2$), which can cause a strong bias in the statistics of precipitation at a local scale, based on inadequate representation of important mesoscale processes, such as convection (IPCC 2012; Cioffi *et al.* 2016). Regional Climate Models (RCMs) derived from downscaled GCMs have better resolution ($<100 \text{ km}^2$). RCMs represent the convective precipitation processes and atmospheric dynamics at a higher resolution than GCMs but also have limited ability to represent local rainfall processes (Takayabu *et al.* 2015). Further downscaling of RCMs by means of statistical or stochastic downscaling techniques is usually required to increase the resolution of climatic information on a local-scale (Garcia-Aristizabal *et al.* 2015). Several previous studies have applied RCMs to study rainfall extremes. Frei *et al.* (2006) used RCM data to study future change of precipitation extremes in Europe, while Garcia-Aristizabal *et al.* (2015) applied RCM precipitation data to conduct extreme value analysis of non-stationary climate-related extreme events in Dar es Salaam, Tanzania.

Studies assessing changes in climate extremes in urban areas of Tanzania are very scarce. Most previous studies in the country have looked at the impacts of climate change on agriculture, livestock and food security (Shemsanga *et al.* 2010; Rowhani *et al.* 2011; Mang'anya 2018), carbon storage in vegetation (Beda 2013), asset exposure to coastal flooding (Kebede & Nicholls 2011), gender equality (Nelson & Stathers 2009), etc. Climate variability in urban areas of Tanzania from the previous research works have studied only the general trend of climatic variables based on mean values. A decreasing trend in the number of rainy days per year in Dar es Salaam over the past five decades has been observed. Also, despite a decline in mean annual rainfall in Dar es Salaam, there has been a random variation in 24-hour maximum rainfall recorded within the past decade (PASS 2011).

In this study, we used ground measured daily rainfall data for the period 1967–2017 from four gauging stations (Figure 1), and the RCM based future daily rainfall data (extracted at the same coordinates) for the period 2018–2050. The data were used to study temporal variability in annual, seasonal and extreme rainfall in the urban catchments of Dar es Salaam for past and future scenarios.

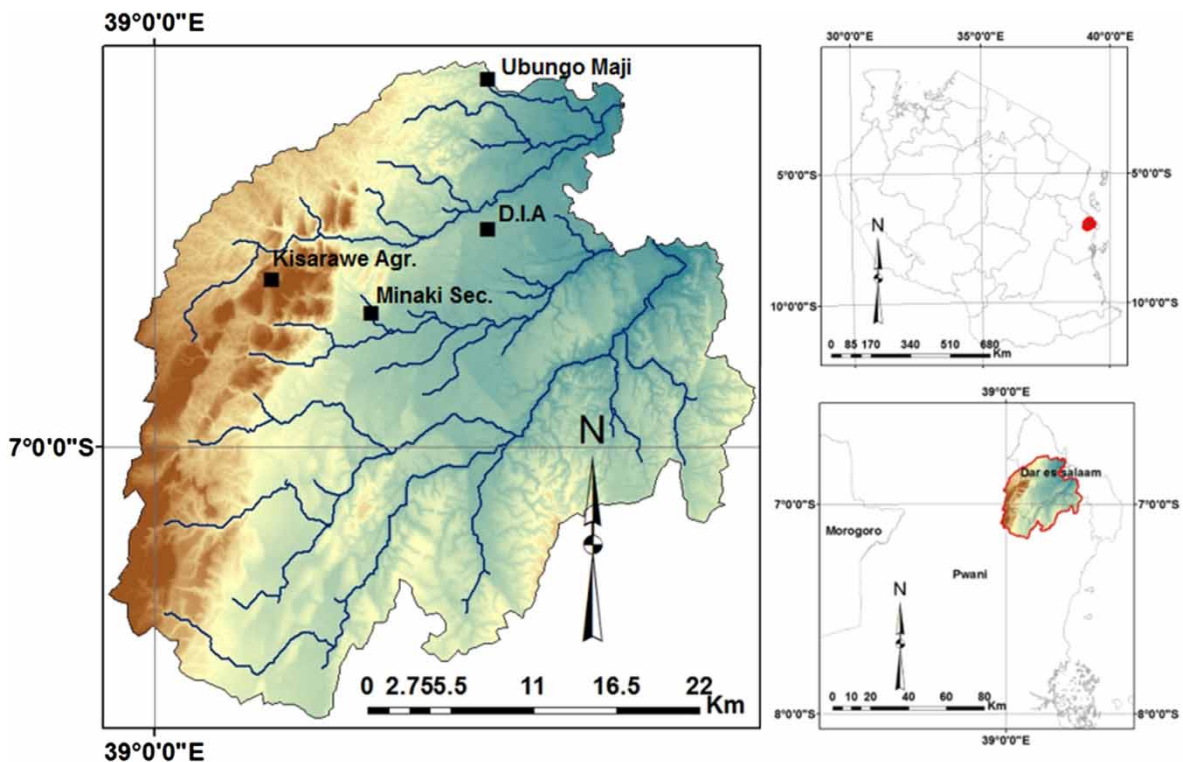


Figure 1 | Study area geographical location within Tanzania.

Specifically, the objectives of this study are: (i) to study and compare trends in annual and seasonal total and maximum rainfall for past and future scenarios and (ii) to determine and compare changes in the intensity and frequency of extreme rainfall between past and future scenarios. Quantification of the changes in magnitudes of annual, seasonal and peak rainfall trends and frequencies of extreme rainfall in the urban catchments of Dar es Salaam fills the gap that was left by previous studies on climate extremes conducted in the region. The significance of this study is based on the fact that its findings could be used to identify long term changes in intensities and frequencies of extreme rainfall which could be an indication of climate change. Also, the results of extreme rainfall frequency analysis and the possible changes in magnitudes are considered vital information for the engineering community based on the fact that the concept of return period is commonly used for the design of urban stormwater infrastructure and flood protection projects.

MATERIALS AND METHODS

Description of the study area

This research was carried out in the selected 1,200 km² study area which is located within Pwani and Dar es Salaam regions in the eastern coastal part of Tanzania, between longitudes 39°01'18.37"–39°28'29.55" E and latitudes 6°35'17.48"–7°59'18.92" S. The area consists of Msimbazi, Kizinga, and Mzinga sub-catchments; reaching 40.2, 29.1, and 58.2 km respectively, starting from the highlands of Pwani region, running through the central urban portion of Dar es Salaam region, and draining the water into the Indian Ocean (Figure 1). Within the study area, the highlands of Pwani are approximately 240 m above sea level; with a peak altitude of 339 m, and they receive an average of 1,200 mm of rainfall annually. The lowlands of the Dar es Salaam region are approximately 57 m above sea level; with the lowest altitude of 15 m, and they receive an average of 1,000 mm of rainfall annually. The area has a bi-modal rainfall distribution; the two main rainy seasons being the long rains and the short rains. The long rains season (Masika) occurs from mid-March to the end of May and the short rains (Vuli) from mid-October to late December (see Figure 2). The study area is characterized by tropical climatic conditions. It is generally hot and humid throughout the year with mean daily temperatures ranging from 26 °C during the coolest season (June–September) to 35 °C during the hot-test season (October–March) (Mahongo & Khamis 2006).

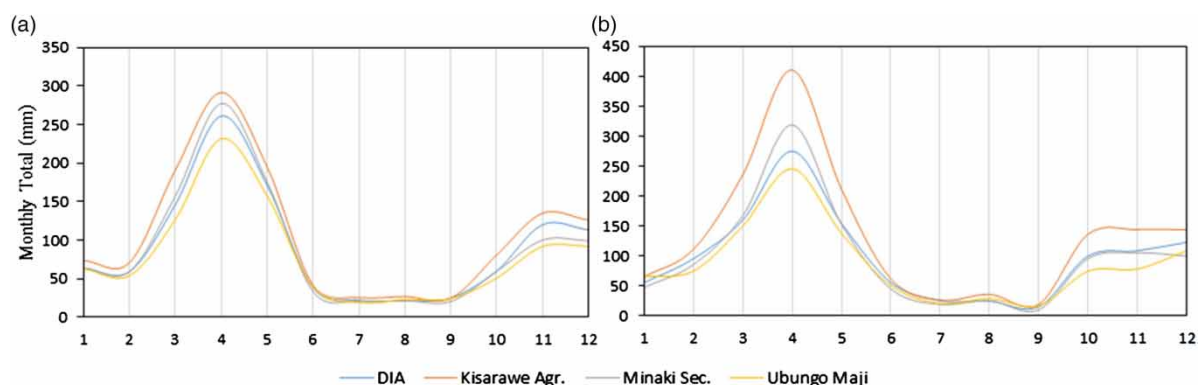


Figure 2 | Mean monthly rainfall distribution: (a) 1967–2017; (b) 2018–2050.

Being the largest commercial, industrial and urban center of Tanzania, Dar es Salaam plays a major role in the country's economic development; contributing to about 16% of the country's gross domestic product (GDP). The major economic activities around the area include tourism, fishing,

forestry, mining and quarrying, and manufacturing. With a fast-growing population and rapid urbanization, the study area has the highest population density in the country, with a density of 3,133 people per square kilometer; and about 70% of the total population live in unplanned areas. These phenomena represent the most fundamental dynamic factors behind most of the immediate causes of environmental degradation (Kebede & Nicholls 2011).

Data

For this study, available historical rainfall data of daily time-step from four gauging stations, i.e. Dar es Salaam International Airport (D.I.A), Kisarawe Agr., Ubungo Maji, and Minaki Sec., were collected from the archives of Tanzania Meteorological Agency (TMA) to assess the trend and frequency of extreme rainfall in the urban catchments of Dar es Salaam, Tanzania for the period 1967–2017 (here referred to as the ‘past scenario’). The Coordinated Regional Modeling Experiment (CORDEX) repository for Africa domain (AFR-44) Regional Climate Model (RCM) (available at <https://esgf-node.llnl.gov/search/esgf-llnl/>) was used to obtain projected rainfall data of daily time-step for the period 2018–2050 (here referred to as the ‘future scenario’). The Representative Concentration Pathway (RCP) 4.5 was used as the criterion for selecting the RCM future daily rainfall data. The RCP4.5 represents a medium-level concentration scenario of greenhouse gas with a radiative forcing of 4.5 Wm^{-2} (equivalent to a CO_2 concentration of 538 ppm) by 2100. The emissions in RCP4.5 are projected to peak around the mid-21st century; around 2040, and projected to decline thereafter (Meinshausen *et al.* 2011). Considering the wide applicability of the RCP4.5 scenario in previous research works (Hsu *et al.* 2013), also because this study intended to look at rainfall projections until the mid-21st century, hence this was the basis for selecting RCP4.5 scenario in this study. Moreover, a mid-level CO_2 concentration scenario was considered a more realistic one since the RCP8.5 concentration scenario has been found to be an extremely high overestimation of fossil fuel usage and it can be interpreted as an implausible scenario (Wang *et al.* 2017; Hausfather & Peters 2020). Furthermore, projection of the RCP4.5 CO_2 concentration scenario of 538 ppm by 2100 already exceeds what is considered a dangerous level of 410 ppm.

The co-ordinates of the four ground rainfall gauging stations in the study area were used in the extraction of the projected rainfall data. Delta method was used for the bias correction of the RCM output while trying to obtain a more realistic projection by representing the effects of the local forcings. Trzaska & Schnarr (2014) and Yazd *et al.* (2019) discuss the Delta method in detail, including its merits and shortcomings relative to other methods of statistical downscaling.

Table 1 shows the statistical properties of the collected rainfall data for both the past and future scenarios (considering days with rainfall ≥ 1 mm). The data sample used in the assessment of rainfall trends contained annual and seasonal totals and peak rainfall series (in seasonal and yearly based blocks) for the stated periods of record in each rainfall station. The data sample used in the assessment of the frequency of extreme rainfall events contained values equal and above a threshold (u) of 40 mm. This was selected as the lowest boundary of extreme rainfall events for both scenarios based on the box plot technique. Despite the threshold for the future scenario being slightly higher (≈ 43 mm), $u = 40$ mm was maintained for consistency and comparison purposes; considering the marginal difference. The rainfall time series were subjected to probability distribution fitting before and after data trimming using the stated threshold. This was necessary in order to identify the candidate probability distribution model to use for extreme rainfall frequency modeling.

The Mann–Kendall test

In this study, the long-term trends in rainfall time series and their significance were tested using the Mann–Kendall (MK) non-parametric method (Mann 1945; Kendall 1975). The MK method was

Table 1 | Descriptive statistics

Data statistic	Station							
	D.I.A		Kisarawe Agr.		Minaki Sec.		Ubungu Maji	
Scenario	Past	Future	Past	Future	Past	Future	Past	Future
Mean	12.77	14.11	14.50	18.25	13.04	14.43	12.93	14.93
Median	6.70	6.98	8.00	9.02	7.60	7.43	7.50	8.27
Variance	253.03	332.53	321.79	568.51	216.70	330.55	227.79	332.54
Std. dev.	15.91	18.24	17.94	23.84	14.72	18.18	15.09	18.24
CV	1.25	1.29	1.24	1.31	1.13	1.26	1.17	1.22
Skewness	2.86	2.82	2.99	2.86	2.59	2.75	2.72	2.80
P25	2.90	2.90	3.50	4.06	3.70	3.44	3.10	3.29
P75	16.20	17.39	18.00	22.52	17.00	17.82	16.60	18.96
P90	32.10	35.48	35.60	46.01	31.51	36.19	30.70	35.63
P95	44.59	52.04	50.00	67.56	42.87	51.94	42.50	50.99
Max.	156.40	165.85	175.00	191.42	129.00	141.09	125.30	150.01
Upper outlier fence	36.15	39.13	39.75	50.21	36.95	39.39	36.85	42.47

CV, coefficient of variation; P, percentile.

preferred over a number of other options for a similar task (e.g. Spearman's Rho, parametric *t*-test, etc.) since it does not assume any particular probability distribution. Also, with the MK method, trend analysis is less influenced by the outliers in the data. The statistical significance of the trends in this study was evaluated at 5% level of significance against the null hypothesis that trend does not exist.

Let x_1, x_2, \dots, x_n be the data points in the time series with n records, and x_j be the data point at time j . Each data point is compared to the subsequent data point. The MK statistic, S , is initially assumed to be zero (no trend). S is then incremented by 1 if the subsequent data are higher than the previous one. Similarly, S is decremented by 1 if the subsequent data are lower than the previous one. The final value of S is the net result of all increments and decrements. The Mann-Kendall, S statistic is calculated as:

$$S = \sum_{k=1}^{n-1} \sum_{j=R+1}^n \text{sign}(X_j - X_k) \quad (1)$$

where

$$\text{sign}(X_j - X_k) = \begin{cases} 1 & \text{if } X_j - X_k > 0 \\ 0 & \text{if } X_j - X_k = 0 \\ -1 & \text{if } X_j - X_k < 0 \end{cases}$$

The trend can be said to be increasing when S is high and positive, and decreasing when it is a very low negative value. To further quantify the statistical significance of the trend, it requires computation of the probability associated with S and the sample size n . Blain (2013) described in detail the procedure to compute the probability associated with S .

For $n \geq 10$, the test statistic S is approximately normally distributed with a mean of zero and a variance of:

$$\text{var}(S) = \frac{n(n-1)(2n+5)}{18} \quad (2)$$

The normal Z-test statistic is calculated as:

$$z = \begin{cases} \frac{S - 1}{\sqrt{\text{Var}(S)}} & \text{if } S > 0 \\ 0 & \text{if } S = 0 \\ \frac{S + 1}{\sqrt{\text{Var}(S)}} & \text{if } S < 0 \end{cases} \quad (3)$$

If $|Z| > Z_{1-\alpha/2}$, the null hypothesis is rejected at α level of significance. A positive value of Z indicates an upward trend and a negative value indicates a downward trend.

Sen's estimator of slope

Theil–Sen's slope estimator (Sen 1968) was used in this study to determine the magnitude of linear trends in the time series of seasonal and annual rainfall. Sen's method calculates the slope of linear trends as a change in measurement per change in time. It is also known as the 'median of pair-wise slopes', and works better than the least-squares regression when the sample size is large (Gocic & Trajkovic 2013). The slope estimates of pairs of data are computed as follows:

$$Q = \frac{X_j - X_k}{j - k} \quad (4)$$

where Q = slope between X_j and X_k ; X_j = data point at time j ; X_k = data point at time k ; j = time after time k .

The median of slope estimates is the Sen's estimator of slope.

Modeling by Generalized Pareto (GP) distribution

Extreme Value Theory (EVT) has been widely applied to analyze and estimate extreme natural events (unusually large or small) commonly using either the Generalized Pareto (GP) or the Generalized Extreme Value (GEV) distributions. EVT is used for derivation of probability distribution of events at the far end of the upper or lower ranges of other probability distributions. It is also used to determine (extrapolate) the probability of occurrence of events outside of the observed data series.

Based on the goodness of fit of the GP distribution to the extreme rainfall data in this study, GP distribution, first introduced by Pickands (1975), was used for modeling the tail values of Gamma distribution (fitted to the original time series). The exceedances over high thresholds (peak over threshold) method was used to obtain extreme rainfall time series. This method was preferred over the maxima over fixed time period (block maxima) method because it provides a more efficient approach for obtaining the maxima time series for GP modeling, and it also produces a longer series and hence increases the modeling accuracy.

Let X be a random variable. The GP distribution functions within three sub-models with their cumulative distribution functions are defined as follows (Reiss & Thomas 2007).

Exponential (GP0), $\alpha = 0$:

$$W_0(x) = 1 - e^{-z}, z \geq 0 \quad (5)$$

Pareto (GP1), $\alpha > 0$:

$$W_{1,\alpha}(x) = 1 - z^{-\alpha}, z \geq 1 \quad (6)$$

Beta (GP2), $\alpha < 0$:

$$W_{2,\alpha}(x) = 1 - (-z)^{-\alpha}, \quad -1 \leq z \leq 0 \quad (7)$$

where $z = (x - \mu) / \sigma$, μ is the threshold or lower bound of X (i.e. a location parameter), σ is a scale parameter, and α is a shape parameter.

By re-parameterizing $\gamma = 1/\alpha$ of GP distribution functions $W_{i,\alpha}$, a unified GP model is obtained as:

$$W_{\gamma}(x) = 1 - (1 + \gamma z)^{-1/\gamma}, \quad \text{for } (1 + \gamma z) \geq 0 \quad (8)$$

Depending on the shape parameter γ , W_{γ} is reduced to Pareto ($\gamma > 0$), Beta ($\gamma < 0$) and Exponential ($\gamma = 0$; which in the limiting sense is interpreted as $\gamma \rightarrow 0$) distributions. XTREMES software was used to implement the above GP distribution functions and model extreme rainfall in this study.

The Maximum Likelihood Estimate (MLE) method was used to estimate the GP distribution parameters. MLE is widely applicable and has shown better adaptability to the extreme value analysis because it provides a consistent approach that can be developed for a variety of estimation situations; therefore, it is considered unbiased. Also, its parameter estimates are normally distributed and have very small variance, i.e. narrow confidence interval. Some of the disadvantages of the MLE method include, it is heavily biased to small samples, and it is very sensitive to the choice of starting value. Zhao *et al.* (2019) described the MLE method in detail. Below is a brief introduction to the MLE method.

Let $f(x; a_1, a_2, \dots, a_m)$ be a probability density function of a random variable X with parameters a_i , $i = 1, 2, \dots, m$, to be estimated. For a random data sample x_1, x_2, \dots, x_n , drawn from this probability density, the joint probability distribution function is defined as:

$$f(x_1, x_2, \dots, x_n; a_1, a_2, \dots, a_m) = \prod_{i=1}^n f(x_i; a_i) \quad (9)$$

Conceptually interpreted as the probability of obtaining a given value of X , say x_i , is proportional to $f(x; a_1, a_2, \dots, a_m)$. Likewise, the probability of obtaining the random sample x_1, x_2, \dots, x_n from the population of X is proportional to the product of the individual probability densities or the joint probability density function. This joint probability density function is called the likelihood function, denoted by L as:

$$L = \prod_{i=1}^n f(x_i; a_1, \dots, a_m) \quad (10)$$

where the parameters a_i are unknown. By maximizing the likelihood that the sample under consideration is the one that would be obtained if n random observations were selected from $f(x; a_1, a_2, \dots, a_m)$, the unknown parameters are determined.

RESULTS AND DISCUSSION

Magnitudes and significance of rainfall trends

The magnitudes of annual and seasonal rainfall trends for the past and future scenarios as determined using the Sen's estimator of slope are as shown in Figure 3. In this first analysis, scenario data were analyzed separately as independent datasets (i.e. the atomistic approach). Following this approach, for the past scenario, the total annual rainfall was observed to be decreasing at three out of the four

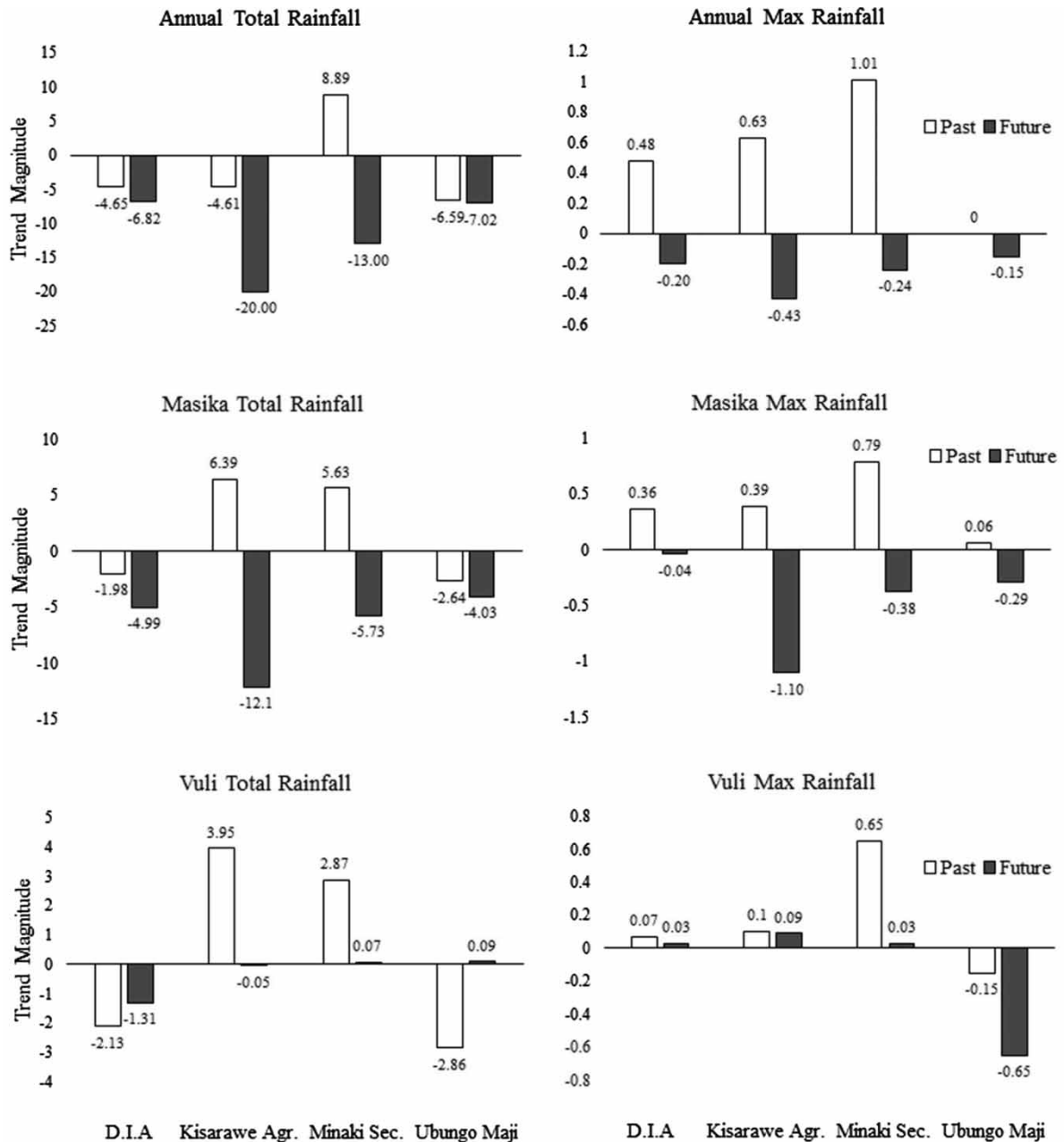


Figure 3 | Variations of annual and seasonal rainfall trend magnitudes for past and future scenarios.

studied stations. The total annual rainfall was observed to be decreasing even further for the future scenario at all the four studied stations. For the future scenario, the highest decrement was observed at the Kisarawe Agr. station, with a 20 mm per year decreasing trend, followed by a 13 mm per year decrement at the Minaki Sec. station. Similarly, the annual maximum rainfall was observed to be decreasing at all the four studied stations in the future scenario. This observation is opposite to what was observed in the past scenario, where annual maximum rainfall was observed to be increasing at three out of the four stations.

As with the annual trend of total and maximum rainfall, the Masika rainfall showed similar characteristics for both total and maximum rainfall in the future scenario compared to the past. Both Masika total and maximum rainfall were observed to be decreasing in the future (with decreasing magnitudes as shown in Figure 3). While annual and Masika maximum rainfall showed opposite characteristics

between past and future scenarios, the Vuli maximum rainfall was observed to maintain a similar trend for the future as it was for the past scenario at all the stations.

Testing of the significance of trend was conducted to ascertain the results of trend magnitudes. This was completed for annual and seasonal total and peak rainfall series. The results of the MK Test Z significance statistic are summarized in Table 2 for both the past and future scenarios. Despite the observation of statistically significant increments in annual maximum rainfall at three out of the four studied stations in the past scenario, none of the stations showed any statistical significance in the observed decrement of annual and seasonal total or maximum rainfall in the future scenario at all the studied stations (following the atomistic approach).

Table 2 | Change in trend significance of rainfall

Scenario	Station							
	D.I.A		Kisarawe Agr.		Minaki Sec.		Ubungu Maji	
	Past	Future	Past	Future	Past	Future	Past	Future
Annual total								
Masika total								
Vuli total								
Annual max.	+		+		+			
Masika max.					+			
Vuli max.								

+: significantly increasing; -: significantly decreasing; no entry: statistically insignificant.

A future decrease in total annual and Masika rainfall (consistent with the results of the atomistic approach analysis in this study) in different parts of Tanzania have also been reported by Cioffi *et al.* (2016). Cioffi *et al.* (2016) also reported a slight decrease in the number of wet days and Masika rainfall, but not for Vuli. A larger decrease in annual rainfall amounts was observed specifically for the Dar es Salaam region. Sappa *et al.* (2015) reported a 20.6% reduction in the recharge of the aquifer in the past 10 years due to reduced infiltration rates in the Dar es Salaam region. The reduction in the infiltration rates was reported due to changes in land cover and the decrease in precipitation. From Figure 2 it can be seen that relative to annual and Masika rainfall, the total Vuli rainfall was not observed to be decreasing in the future (except for the D.I.A station). This observation is also in line with the findings of Cioffi *et al.* (2016). From a global perspective, a decrease in future total annual rainfall has been reported by several studies. Hossain *et al.* (2017) reported a decrease in overall rainfall in Bangladesh, a trend that is projected to continue into the future. Al-Ansari *et al.* (2014) also reported a similar trend for Iraq. These findings are only consistent with the analysis results of the atomistic approach in this study. The analysis of a holistic approach is discussed in the following section of this paper.

Overall magnitudes and significance of rainfall trends

It was of interest to study the behavior of annual and seasonal rainfall trends when the data for past and future scenarios were not treated as independent sets of data, but as a single dataset (i.e. the holistic approach). The overall magnitudes of annual and seasonal rainfall trends when considering the 1967–2050 rainfall time series as one set of data are as shown in Figure 4. It can be seen from Figure 4 that the results of rainfall trend magnitudes show a significant difference from the previous analysis when past and future scenarios were treated independently. The major difference being the annual and seasonal maximum rainfall showed positive trends at all the studied stations. Stations at higher altitudes were observed to experience a larger increase of annual and seasonal peak rainfall than

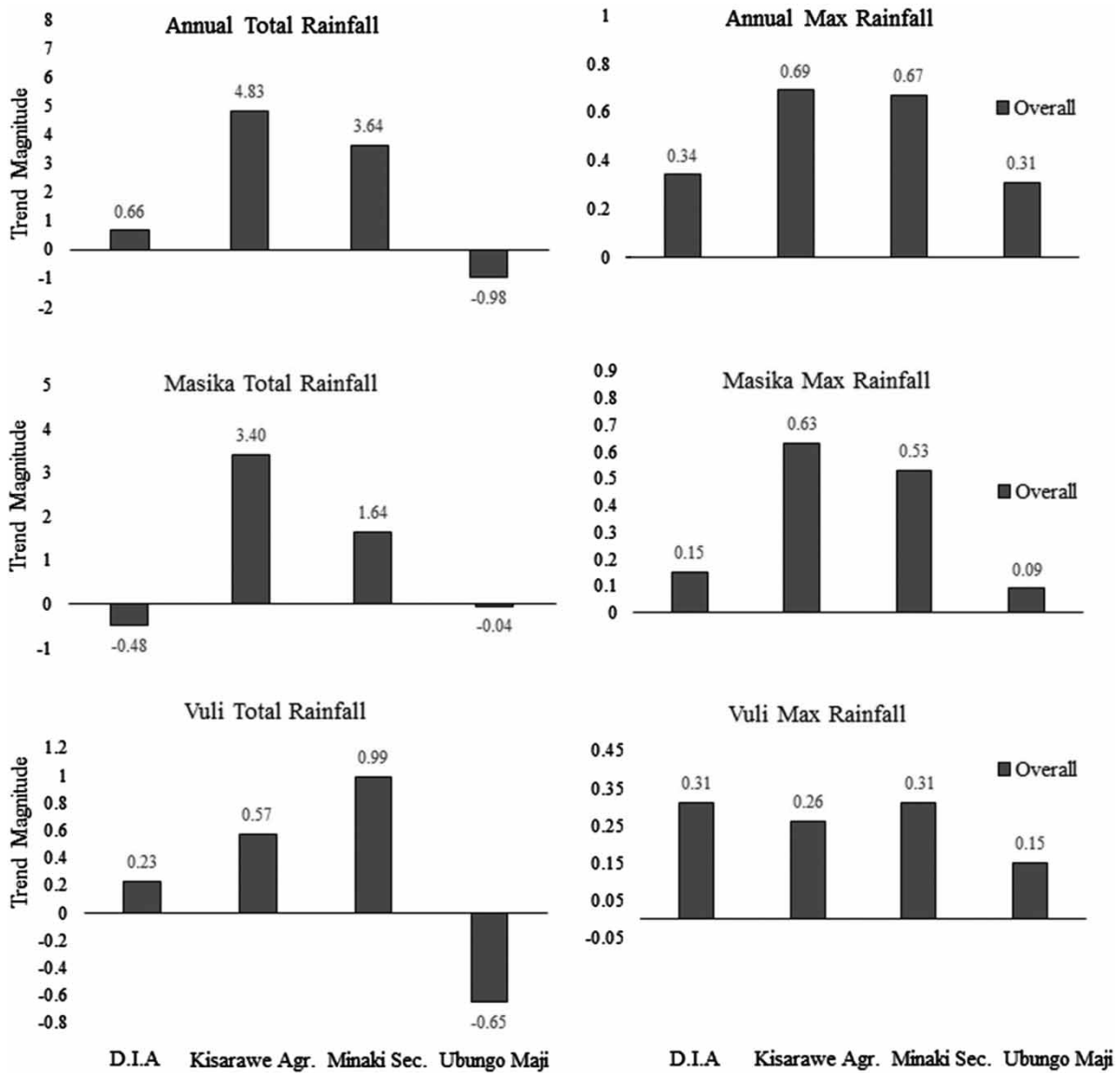


Figure 4 | Overall trend magnitudes of annual and seasonal rainfall.

stations at lower altitudes; having magnitudes of almost double the stations in lower areas. The increase of annual maximum rainfall was found to be statistically significant at all four stations (Table 3). The increase of Masika maximum rainfall was found to be statistically significant at the

Table 3 | Overall trend significance of annual and seasonal rainfall

	Station			
	D.I.A	Kisarawe Agr.	Minaki Sec.	Ubungo Maji
Annual total				
Masika total		+		
Vuli total				
Annual max.	+	+	+	+
Masika max.		+	+	
Vuli max.	+			

+: significantly increasing; -: significantly decreasing; no entry: statistically insignificant.

two stations located in the higher altitudes of the catchments. Trend results for annual and seasonal rainfall totals could not be clearly defined in the holistic approach. An increase of total annual and seasonal rainfall was observed for the higher altitude stations, but the statistical significance test showed an increase of Masika total rainfall was significant only at Kisarawe Agr. station (Table 3). In general, no definitive trend was observed for annual and seasonal rainfall totals, despite indications of a decline in total annual and seasonal rainfall for stations in lowland areas and vice-versa for the ones in the highland areas.

Results of increased annual extreme rainfall for Tanzania in general, observed by Cioffi *et al.* (2016), are consistent with analysis results of the holistic approach in this study but in contradiction with the results of the atomistic approach. In the atomistic approach, extreme rainfall was observed to decrease within a particular block of a data series (i.e. data from the future scenario alone) without considering the influence of data outside that block (i.e. past data); therefore, one needs to be specific when drawing conclusions in such a case. Higher annual variability of extreme rainfall was observed when looking at a larger regional scale of East Africa; this was said to be associated with the complex topographical nature and relief features of the region (Kotir 2011; Fer *et al.* 2017; Mpelasoka *et al.* 2018; Gebrechorkos *et al.* 2019b). Bigi *et al.* (2018) projected an increase of precipitation in the future with exacerbation of floods in Niger, West Africa. While Emmanuel *et al.* (2019) observed high variability of annual rainfall in the future, with higher peaks during wet seasons in the Mono river basin, Benin and Togo. These findings are in line with the findings of the holistic approach of this study.

It was observed in this study that trend results vary significantly depending on the range selection of the rainfall time series. The disparities in extreme rainfall trends can be seen in Figure 5 based on either inclusion or exclusion (i.e. data range selection) of extreme rainfall data. It was found that looking at extreme rainfall data of past and future scenarios separately or as a whole showed contrasting results, as discussed above. When studying the data separately/independently, the extreme rainfall data for the past scenario showed an increasing trend while that of the future scenario showed a decreasing trend despite the finding of increased intensities of extreme rainfall in the future (comparing the 95th percentile line of extreme rainfall for past and future data in Figure 5). Therefore, the

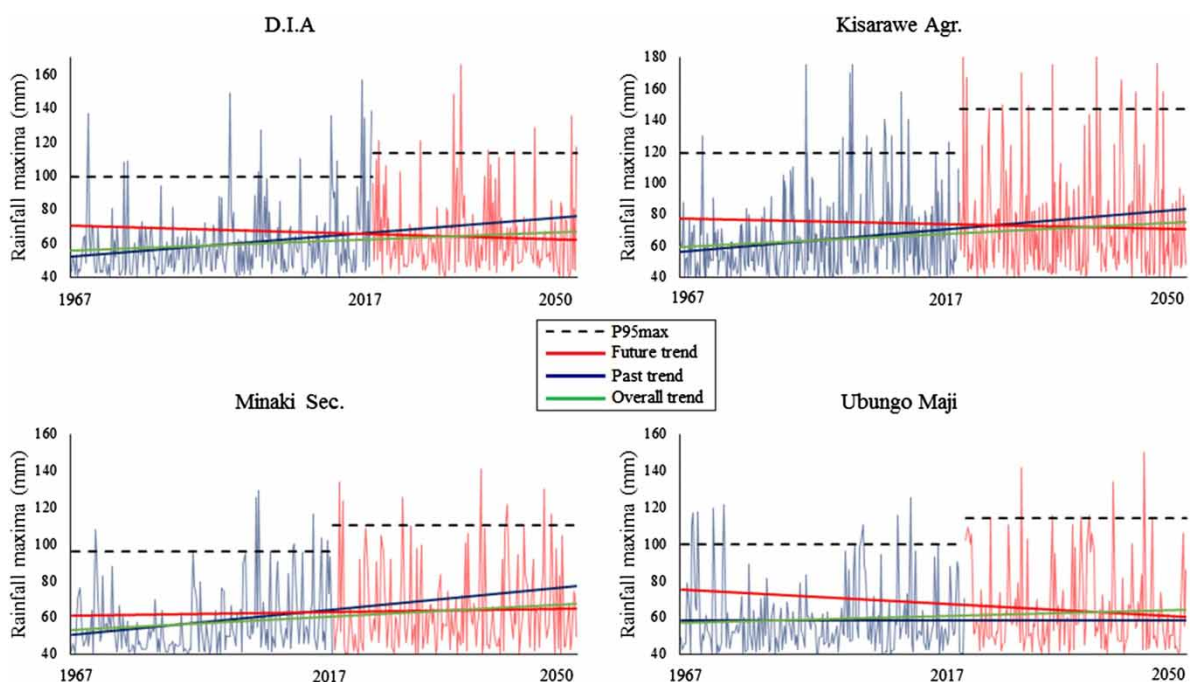


Figure 5 | Disparities in extreme rainfall trends due to data composition or decomposition.

trend results of extreme rainfall made more sense when studying future maximum rainfall relative to the past data (i.e. the results of the holistic approach); rather than treating future data as a totally independent scenario. This is because, if extreme rainfall was observed to be increasing in the past and the intensities of extreme rainfall were observed to be increasing in the future, then one would not expect a long term decreasing trend of extreme rainfall, as one would have concluded following the atomistic approach alone (which could be misleading). On the contrary, for practical application purposes, it was sensible to treat the future extreme rainfall data as an independent dataset when studying extreme rainfall return periods (frequencies of extreme rainfall) in the future and then compare to those of the past. This is because stormwater conveying structures are required to accommodate future storm magnitudes irrespective of the past record. The discussion in the next section is based on this perspective.

Change in extreme rainfall intensities and frequencies

The rainfall time series were subjected to probability distribution fitting before and after extracting the extreme maxima values. Using the graphical approach, the Gamma distribution was observed to be the best fit for rainfall data before trimming the extreme maxima (i.e. when considering a complete set of rainfall data (≥ 1 mm)). After trimming the data and extracting the extreme maxima using the $x \geq 40$ mm criterion, and repeating the probability distribution fitting, the extracted data points were observed to best fit the GP distribution. Extracted sample sizes (n) of extreme maxima from daily rainfall data for each gauging station are shown in Figure 6. Figure 6 also shows the distribution of extreme rainfall values for the past and future scenarios. Looking at both the IQR (Interquartile Range) and 1.5IQR envelopes and comparing the two scenarios, it is evident that in the future the

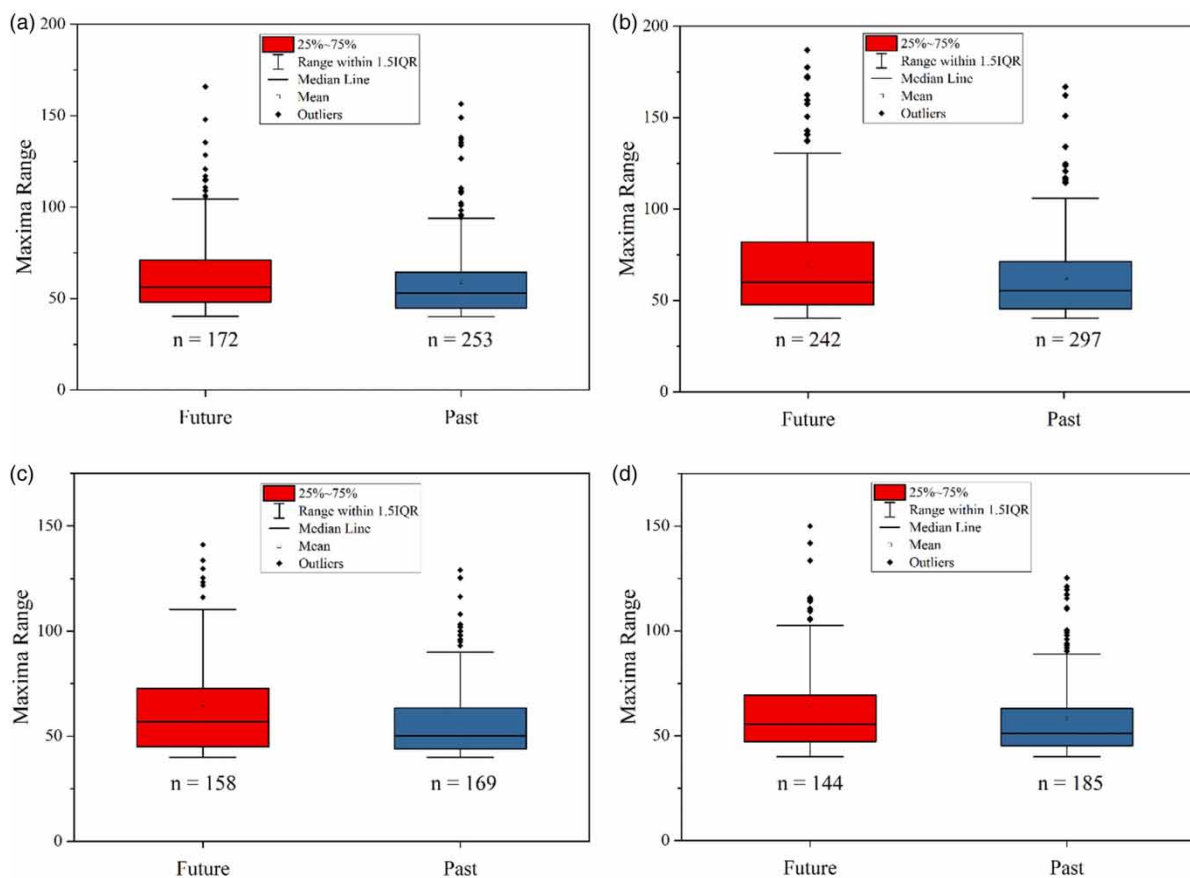


Figure 6 | Change in the distribution of extreme rainfall values for the past and future scenarios at (a) D.I.A, (b) Kisarawe Agr., (c) Minaki Sec., and (d) Ubungu Maji stations.

intensities of extreme rainfall in the study area are expected to increase considerably compared to the past. The future intensities of extreme rainfall were observed to increase between approximately 20 and 25% relative to the past (see Figure 6). Intensification of future extreme rainfall events due to global warming has been reported by several previous studies worldwide (Manola *et al.* 2018; Alex *et al.* 2019; Myhre *et al.* 2019). The reported intensification of future extreme rainfall from previous studies ranges between 10 and 50% depending on the location, model(s) used and emission scenario(s) (Bador & Donat 2018; Donat *et al.* 2019). Knowledge of future frequency and intensity of extreme rainfall is far less established in warmer climates (Myhre *et al.* 2019), therefore the findings of this study can be considered vital in reducing that gap in knowledge.

Testing of the independence of the extracted values of rainfall extremes was performed using the sample autocorrelation plots (not shown for the sake of brevity), and no correlation between extreme rainfall events was observed in the data sample. GP distribution parameters were estimated using the MLE method. From the estimates of the shape parameter (γ), it was observed that $\gamma > 0$ for all the stations, except D.I.A where $\gamma < 0$ in the future scenario (see Figure 7). This implied that the extracted data sample is predominantly in the Pareto distribution sub-model of the GP model as demonstrated by Equations (5)–(8). This observation was also supported by the results of the sample mean excess plots (not shown), which displayed a positive linear trend for all the gauging stations. The mean excess plots were also useful for checking the appropriateness of the selected threshold (u). The linearity of the mean excess plots was an indication of a properly selected u . When generally comparing the estimates of the GP parameters; with a fixed location parameter ($\mu = 40$), the shape parameter (γ) was observed to decrease in the future scenario, while the scale parameter (σ) was observed to increase (see Figure 7). Based on the observed variations of γ and σ , it indicated a change in the shape and behavior of the GP distribution. The estimated $\gamma < 0$ in the future scenario for D.I.A station could have been influenced by the substantial difference in the sample sizes (n) between the past and future scenarios.

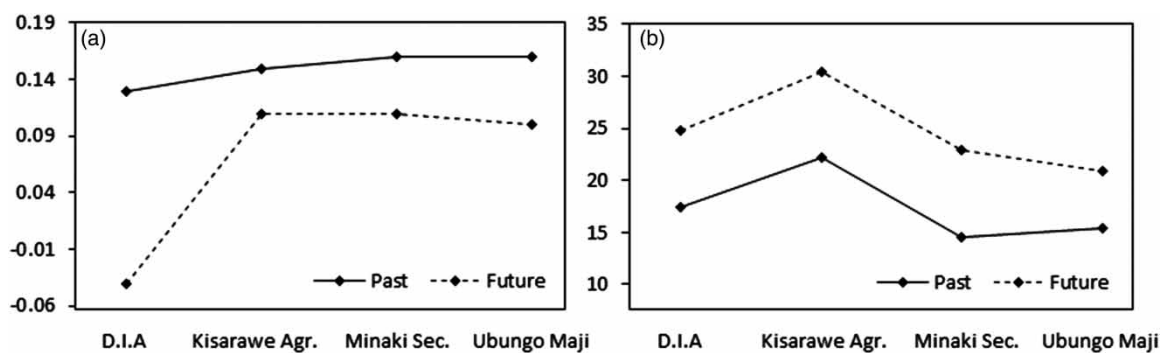


Figure 7 | Non-stationarity in the distribution parameters: (a) γ ; (b) σ .

A visual evaluation of the Quantile-Quantile plots (not shown) revealed that, in general, the GP model performed reasonably adequately in modeling extreme rainfall events for both the past and future scenarios. It was observed that the model performed exceptionally well for the lower values of extreme events, and performed satisfactorily for the events at the far right end of the tail (i.e. the most extreme values). Model performance was statistically ascertained by determining the coefficients of determination (R^2) between the model results and the measured/projected values. R^2 values were found to be over 0.9 in all scenarios; this indicated an adequate performance of the GP model.

Estimated return periods of extreme rainfall events in the study area for past and future scenarios and their comparisons are shown in Figure 8. Due to the previous observation of an increase in the intensities of extreme rainfall in the future scenario relative to the past (Figure 6), for the same return

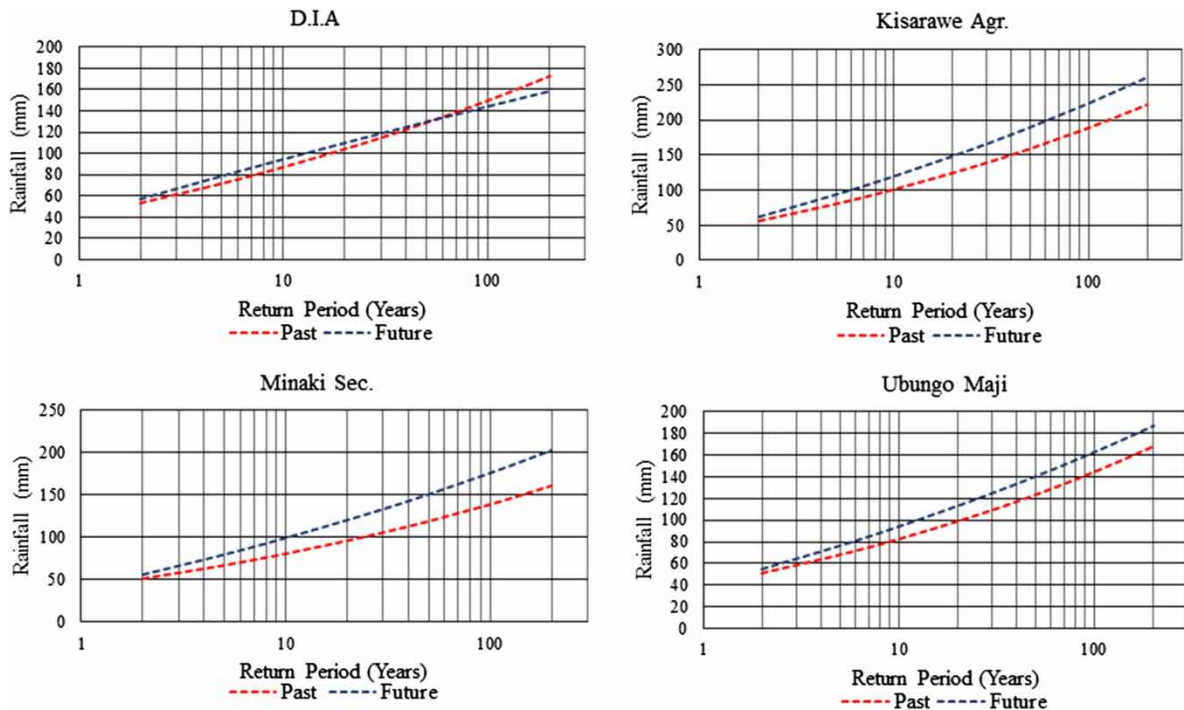


Figure 8 | Extreme rainfall frequencies for past and future scenarios.

period (past and future) the estimated magnitudes of rainfall maxima have increased considerably for all the stations except D.I.A (see Figure 8). From the engineering design perspective, hydraulic structures (i.e. bridges, culverts, drainage channels, sewers, etc.) are usually designed using peak rainfall events with return periods of at least 25 years. It was found in this study that in the past scenario, on average, an event with 100 mm/day intensity was considered a 25-year event, while for the future scenario, on average, an event with 125 mm/day intensity will be considered a 25-year event (see Figure 8). Therefore, with the existing drainage system and flooding conditions in the study area, the situation will only get worse if no measures are taken to improve the stormwater systems and flood control in the future due to the increased frequency and magnitudes of extreme rainfall events observed in this study.

The finding of future increase in peak rainfall intensities was crucial for the case of Dar es Salaam urban flooding. Although other factors may play a role in urban flooding, including land cover conditions, poor drainage system, poor management of solid waste, antecedent soil moisture, etc., rainfall remains the major driving force for surface water runoff generation. A combination of the above mentioned factors can only intensify the flooding problem. Dar es Salaam urban land cover was observed to be greatly modified since 1979; turning from thick vegetated land towards becoming barren land (Mzava *et al.* 2019). This change was observed to be continuous, and about 66.1% of the urban area will consist of built-up land cover by 2030. This type of land cover is characterized by very low to zero water permeability. Therefore, the projected change in land cover and the findings of increased future peak rainfall intensities and frequency from this study will alter the hydrologic response of the studied catchments and more likely will cause increased surface water runoff and the chances of flooding in the study area will increase.

CONCLUSIONS

The results obtained from this study show an indication of climate change. According to the findings of this study, the study area has the possibility of experiencing more frequent and intensive extreme

rainfall in the future. The intensity of future extreme rainfall was observed to increase between approximately 20 and 25% relative to the past; which may lead to more severe floods in the Dar es Salaam urban area. The results of the analysis of extreme rainfall frequency from this study are crucial information for the civil engineering community when designing hydraulic (stormwater carrying) structures in the study area in the future. Currently, it is evident that the flood protection infrastructure in place does not have the capacity to accommodate existing flood magnitudes. According to the findings of this study, these magnitudes will become even larger in the future, therefore improved engineering designs and mitigation strategies are necessary for better management of flooding impacts in the Dar es Salaam urban area.

This study examined the future characteristics of extreme rainfall based on the RCP4.5 CO₂ concentration scenario alone. There is a need for further studies to investigate future behaviors of extreme rainfall under a wider range of CO₂ concentration scenarios and a longer period of time while comparing multiple climate models. Moreover, this study examined rainfall characteristics at a daily time step, although sub-daily rainfall data may behave significantly different from daily data. Therefore, depending on data availability, it is recommended that sub-daily extreme rainfall data be examined in relation to urban flooding in future studies.

ACKNOWLEDGEMENTS

The authors are grateful to the German Academic Exchange Service (DAAD) for financial support and the University of Dar es Salaam (UDSM) for being the host institution while conducting this research.

DATA AVAILABILITY STATEMENT

All relevant data are included in the paper or its Supplementary Information.

REFERENCES

- Al-Ansari, N., Abdellatif, M., Ezeelden, M., Ali, S. S. & Knutsson, S. 2014 Climate change and future long-term trend of rainfall at North-East of Iraq. *J. Civ. Eng. Architect.* **8** (6), 790–805.
- Alex, N., Jesse, K. & Neoline, N. 2019 Evaluation of past and future extreme rainfall characteristics over eastern Uganda. *J. Environ. Agric. Sci.* **18**, 38–49.
- Bador, M. & Donat, M. G. 2018 Assessing the robustness of future extreme precipitation intensification in the CMIP5 ensemble. *J. Clim.* **31**, 6505–6525. <https://doi.org/10.1175/JCLI-D-17-0683.1>.
- Beda, G. 2013 *Carbon Storage Potential and Climate Change Mitigation: A Case of Pugu Forest Reserve, Kisarawe District, Tanzania. M.Sc. Dissertation*, Sokoine University of Agriculture, Tanzania. Available from: www.suaire.suanet.ac.tz:8080/xmlui/bitstream/handle/123456789/513/GOODLUCK%20BEDA.pdf?sequence=1&isAllowed=y.
- Bigi, V., Pezzoli, A. & Rosso, M. 2018 Past and future precipitation trend analysis for the city of Niamey, Niger: an overview. *Climate* **6** (73). <https://doi.org/10.3390/cli6030073>.
- Blain, G. C. 2013 The Mann–Kendall test: the need to consider the interaction between serial correlation and trend. *Acta Sci. Agron.* **35** (4), 393–402.
- Cioffi, F., Conticello, F. & Lall, U. 2016 Projecting changes in Tanzania rainfall for the 21st century. *Int. J. Climatol.* **36**, 4297–4314.
- Donat, M. G., Angelil, O. & Ukkola, A. M. 2019 Intensification of precipitation extremes in the world's humid and water-limited regions. *Environ. Res. Lett.* **14**, 065003. <https://doi.org/10.1088/1748-9326/ab1c8e>.
- Elleder, L. 2015 Historical changes in frequency of extreme floods in Prague. *Hydrol. Earth Syst. Sci.* **19**, 4307–4315.
- Emmanuel, L. A., Houngue, N. R., Biaou, C. A. & Badou, D. F. 2019 Statistical analysis of recent and future rainfall and temperature variability in the Mono river watershed (Benin, Togo). *Climate* **7** (8). <https://doi.org/10.3390/cli7010008>
- Erman, A., Tariverdi, M., Obolensky, M., Chen, X., Vincent, R. C., Malgioglio, S., Rentschler, J., Hallegatte, S. & Yoshida, N. 2019 *The Role of Poverty in Exposure, Vulnerability and Resilience to Floods in Dar es Salaam*. World Bank Group.

- Available from: <http://documents.worldbank.org/curated/pt/788241565625141093/pdf/Wading-Out-the-Storm-The-Role-of-Poverty-in-Exposure-Vulnerability-and-Resilience-to-Floods-in-Dar-Es-Salaam.pdf>.
- Fer, I., Tietjen, B., Jeltsch, F. & Wolff, C. 2017 The influence of El Niño-Southern Oscillation regimes on eastern African vegetation and its future implications under the RCP8.5 warming scenario. *Biogeosciences* **14** (18), 4355–4374. <https://doi.org/10.5194/bg-14-4355-2017>.
- Frei, C., Scholl, R., Fukutome, S., Schmidli, J. & Vidale, P. L. 2006 Future change of precipitation extremes in Europe: Intercomparison of scenarios from regional climate models. *J. Geophys. Res.* **111**, D06105. <https://doi.org/10.1029/2005JD005965>.
- García-Aristizabal, A., Bucchignani, E., Palazzi, E., D'Onofrio, D., Gasparini, P. & Marzocchi, W. 2015 Analysis of non-stationary climate-related extreme events considering climate change scenarios: an application for multi-hazard assessment in the Dar es Salaam region, Tanzania. *Nat. Hazards* **75**, 289–320. <https://doi.org/10.1007/s11069-014-1324-z>.
- Gautam, R. C. & Bana, R. S. 2014 Drought in India: its impact and mitigation strategies – a review. *Indian J. Agron.* **59** (2), 179–190.
- Gebrechorkos, S. H., Hulsmann, S. & Bernhofer, C. 2019a Long-term trends in rainfall and temperature using high-resolution climate datasets in East Africa. *Sci. Rep.* **9**, 11376.
- Gebrechorkos, S. H., Hulsmann, S. & Bernhofer, C. 2019b Changes in temperature and precipitation extremes in Ethiopia, Kenya, and Tanzania. *Int. J. Climatol.* **39**, 18–30. <https://doi.org/10.1002/joc.5777>.
- Gocic, M. & Trajkovic, S. 2013 Analysis of changes in meteorological variables using Mann–Kendall and Sen's slope estimator statistical tests in Serbia. *Global Planet. Change* **100**, 172–182.
- Hausfather, Z. & Peters, G. P. 2020 Emission – the 'business as usual' story is misleading. *Nature* **577** (7792), 618–620. <https://doi.org/10.1038/d41586-020-00177-3>.
- Hossain, M. M., Hasan, M. Z., Alauddin, M. & Akhter, S. 2017 Historical and future rainfall variations in Bangladesh. *Int. J. Environ. Ecol. Eng.* **11** (7), 694–699.
- Hsu, P., Li, T., Murakami, H. & Kitoh, A. 2013 Future change of the global monsoon revealed from 19 CMIP5 models. *J. Geophys. Res.* **118**, 1247–1260.
- IPCC 2012 *Managing the Risks of Extreme Events and Disasters to Advance Climate Change Adaptation*. Cambridge University Press, Cambridge, MA.
- IPCC 2013 Climate Change 2013: the physical science basis. In: *Contribution of Working Group I to the Fifth Assessment Report of the Intergovernmental Panel on Climate Change*. Cambridge University Press, Cambridge, MA.
- Kebede, A. S. & Nicholls, R. J. 2011 *Population and Assets Exposure to Coastal Flooding in Dar es Salaam (Tanzania): Vulnerability to Climate Extremes Report*. Global Climate Adaptation Partnership (GCAP) Programme. University of Southampton, UK.
- Kendall, M. G. 1975 *Rank Correlation Measures*. Charles Griffin, London.
- Kijazi, A. L. & Reason, C. R. C. 2009 Analysis of the 2006 floods over northern Tanzania. *Int. J. Climatol.* **29**, 955–970.
- Kotir, J. H. 2011 Climate change and variability in sub-Saharan Africa: a review of current and future trends and impacts on agriculture and food security. *Environ. Dev. Sustainable* **13** (3), 587–605. <https://doi.org/10.1007/s10668-010-9278-0>.
- Li, G., Zhang, X., Cannon, A. J., Murdock, T., Sobie, S., Zwiers, F., Anderson, K. & Qian, B. 2018 Indices of Canada's future climate for general and agricultural adaptation applications. *Clim. Change* **148**, 249–263.
- Mahongo, S. B. & Khamis, O. I. 2006 *The Tanzania National Sea Level Report*. Tanzania Fisheries Research Institute and the Department of Survey and Urban Planning. Dar es Salaam, Tanzania. Available from: www.gloss-sealevel.org/publications/documents/tanzania2006.pdf.
- Mallakpour, I. & Villarini, G. 2015 The changing nature of flooding across the central United States. *Nat. Clim. Change* **5**, 250–254.
- Mang'anya, E. 2018 The impacts of climate change on food security in Tanzania: a case study of Kilosa District. *J. Geogr. Assoc. Tanzania* **39** (1), 173–188.
- Mann, H. B. 1945 Non-parametric tests against trend. *Econometrica* **13**, 245–259.
- Manola, I., Hurk, B., De Moel, H. & Aerts, J. C. J. H. 2018 Future extreme precipitation intensities based on a historic event. *Hydrol. Earth Syst. Sci.* **22**, 3777–3788. <https://doi.org/10.5194/hess-22-3777-2018>.
- Meinshausen, M., Smith, S. J., Calvin, K., Daniel, J. S., Kainuma, M. L. T., Lamarque, J. F., Matsumoto, K., Montzka, S. A., Raper, S. C. B., Riahi, K., Thomson, A., Velders, G. J. M. & van Vuuren, D. P. P. 2011 The RCP greenhouse gas concentrations and their extensions from 1765 to 2300. *Clim. Change* **109**, 213–241.
- Mpelasoka, F., Awange, J. L. & Zerihun, A. 2018 Influence of coupled ocean-atmosphere phenomena on the Greater Horn of Africa droughts and their implications. *Sci. Total Environ.* **610–611** (Suppl. C), 691–702. <https://doi.org/10.1016/j.scitotenv.2017.08.109>.
- Myhre, G., Alterskjaer, K., Stjern, C. W., Hodnebrog, Ø., Marelle, L., Samset, B. H., Sillmann, J., Schaller, N., Fischer, E., Schulz, M. & Stohl, A. 2019 Frequency of extreme precipitation increases extensively with event rareness under global warming. *Sci. Rep.* **9**, 16063. <https://doi.org/10.1038/s41598-019-52277-4>.
- Mzava, P., Nobert, J. & Valimba, P. 2019 Land cover change detection in the urban catchments of Dar es Salaam, Tanzania using remote sensing and GIS techniques. *Tanz. J. Sci.* **45** (3), 315–329.
- Nangombe, S., Zhou, T., Zhang, W., Wu, B., Hu, S., Zou, L. & Li, D. 2018 Record-breaking climate extremes in Africa under stabilized 1.5°C and 2.0°C global warming scenarios. *Nat. Clim. Change* **8** (5), 375–380.

- Nelson, V. & Stathers, T. 2009 Resilience, power, culture, and climate: a case study from semi-arid Tanzania, and new research directions. *Gend. Dev.* **17** (1), 1–14.
- Ngailo, T. J., Reuder, J., Rutalebwa, E., Nyimvua, S. & Mesquita, M. 2016 Modelling of extreme maximum rainfall using extreme value theory for Tanzania. *Int. J. Sci. Innov. Math. Res.* **4** (3), 34–45.
- Otto, F. E. L. 2017 Attribution of weather and climate events. *Ann. Rev. Environ. Resour.* **42**, 627–646.
- Pan-African START Secretariat (PASS) 2011 *A Report on Urban Poverty & Climate Change in Dar es Salaam, Tanzania: A Case Study*. Ardhi University, Tanzania. Available from: https://start.org/wp-content/uploads/dar-case-study_p1-65_compressed.pdf.
- Pickands, J. 1975 Statistical inference using extreme order statistics. *Ann. Stat.* **3**, 119–131.
- Reiss, R. D. & Thomas, M. 2007 *Statistical Analysis of Extreme Values: With Applications to Insurance, Finance, Hydrology and Other Fields*, 3rd edn. Birkhauser, Basel, Switzerland, p. 511.
- Rowhani, P., Lobell, D. B., Linderman, M. & Ramankutty, N. 2011 Climate variability and crop production in Tanzania. *Agric. For. Meteorol.* **151**, 449–460.
- Sakijege, T., Lupala, J. & Sheuya, S. 2012 Flooding, flood risks and coping strategies in urban informal residential areas: the case of Keko Machungwa, Dar es Salaam, Tanzania. *J. Disaster Risk Stud.* **4** (1), 46–55.
- Sappa, G., Trotta, A. & Vitale, S. 2015 *Climate Change Impacts on Groundwater Active Recharge in Coastal Plain of Dar es Salaam (Tanzania)*. Springer International Publishing, Switzerland.
- Sen, P. K. 1968 Estimation of the regression coefficient based on Kendall's tau. *J. Am. Stat. Assoc.* **63**, 1379–1389.
- Shemsanga, C., Omambia, A. N. & Gu, Y. 2010 The cost of climate in Tanzania: impacts and adaptations. *J. Am. Sci.* **6** (3), 182–196.
- Takayabu, I., Hibino, K., Sasaki, H., Shiogama, H., Mori, N., Shibutani, Y. & Takemi, T. 2015 Climate change effects on the worst-case storm surge: a case of Typhoon Haiyan. *Environ. Res. Lett.* **10**, 064011. <https://doi.org/10.1088/1748-9326/10/6/064011>.
- Trzaska, S. & Schnarr, E. 2014 *A Review of Downscaling Methods for Climate Change Projections*. Tetra Tech ARD, USAID, Burlington, Vermont.
- Wang, J., Feng, L., Tang, X., Bentley, Y. & Hook, M. 2017 The implications of fossil fuel supply constraints on climate change projections: a supply-side analysis. *Futures* **86** (2), 58–72. <https://doi.org/10.1016/j.futures.2016.04.007>.
- Yazd, H. R. G., Salehnia, N., Kolsouni, S. & Hoogenboom, G. 2019 Prediction of climate variables by comparing the K-nearest neighbor method and MIROC5 outputs in an arid environment. *Clim. Res.* **77**, 99–144.
- Zhao, X., Zhang, Z., Cheng, W. & Zhang, P. 2019 A new parameter estimator for the generalized Pareto distribution under the peaks over threshold framework. *Mathematics* **7**, 406–423.

First received 29 January 2020; accepted in revised form 26 June 2020. Available online 8 August 2020